Int. J. Electron. Commun. (AEÜ) 81 (2017) 50–55

Contents lists available at ScienceDirect

International Journal of Electronics and Communications (AEÜ)

journal homepage: www.elsevier.com/locate/aeue

Regular paper

A covariance matrix shrinkage method with Toeplitz rectified target for DOA estimation under the uniform linear array

Yanyan Liu [a], Xiaoying Sun [a,*], Shishun Zhao [b]

[a] Department of Communication Engineering of Jilin University, Changchun, Jilin 130025, China
[b] Department of Mathematics of Jilin University, Changchun, Jilin 130022, China

ARTICLE INFO

Article history:
Received 23 October 2016
Accepted 23 June 2017

Keywords:
Direction of arrival (DOA) estimation
Covariance matrix estimation
Shrinkage estimation
MUSIC
Random matrix theory

ABSTRACT

A covariance matrix shrinkage method is proposed to make an improvement of the direction of arrival (DOA) estimation under a uniform linear array in a scenario where the number of sensors is large and the sample size is relatively small. The main contribution is that we provide a shrinkage target with Toeplitz structure and deduce a closed-form estimation of the shrinkage coefficient. The closed-form and the expectation of the shrinkage coefficient estimate are calculated based on the unbiased and consistent estimates of the trace and moments of a Wishart distributed covariance matrix. The statistical property of the shrinkage coefficient estimate is discussed through theoretical analysis and simulations, which demonstrate the shrinkage coefficient estimate can ensure that the proposed covariance matrix estimate is a good compromise between the sample covariance matrix (SCM) and the target. The root-mean-square-error (RMSE) simulations of DOA estimation show that the proposed method can improve the multiple signal classification (MUSIC) DOA estimation performance in the case of low signal-to-noise ratio (SNR) with small sample size, and also can provide a satisfactory performance at high SNR.

1. Introduction

Direction-of-arrival (DOA) estimation of signal sources is a fundamental topic in signal processing and widely applied in communications, radar and sonar, etc. [1,2]. The subspace-based DOA estimation methods including multiple signal classification (MUSIC) algorithm and the modified versions are referred to as super-resolution techniques in the case of high signal-to-noise ratio (SNR) with sufficient samples, which offer a good compromise between resolution and computational complexity [3,4]. They obtain the signal and noise subspaces through the eigenvalue decomposition of the sample covariance matrix (SCM). The SCM in these methods is usually estimated by the maximum likelihood estimation, which is a well estimation when the sample size is much lager than the dimension. However, in certain scenarios, the number of available samples N may be restricted and is on the same order of magnitude as the number of sensors M. For example, when signals are short-time stationary processes, or an array system contains a large number of sensors in the multiple-input multiple-out (MIMO) radar system. In these cases, the SCM is not a good estimation of the true covariance matrix any more, which leads to the subspace-based DOA estimation methods perform poorly [5].

The general asymptotic situation, where $M, N \rightarrow \infty$ with $M/N \rightarrow c \in (0, \infty)$, can provide a more accurate description for the practical scenario in which M and N are the finite with comparable values [6]. X. Mestre analyzed the asymptotic behavior of the eigenvalues and eigenvectors of the SCM by Stieltjes transform, and proved that the traditional sample estimates are inconsistent and indicate a poor performance in the general asymptotic situation [7]. His team modified the subspace algorithms for DOA estimation (their methods are named as G-MUSIC and G-SSMUSIC) based on their improved estimation of the eigenvalues and eigenvectors [8]. Compared with the conventional subspace methods, X. Mestre et al. focused on providing new estimations of the quadratic form of the eigenvectors and improving the resolution of DOA estimation by weighting the sample eigenvector projection matrices. From another perspective, it will be an effective way to obtain good DOA estimates via improving the estimation of the covariance matrix when N is relatively small compared with M.

Covariance matrix shrinkage estimation algorithms are suitable for high dimensional problems with relatively few samples (large M and small N), and the estimate realizes a good compromise between the SCM and a well-conditioned matrix (the

* Corresponding author.
E-mail addresses: liuyyjany@126.com (Y. Liu), sunxy@jlu.edu.cn (X. Sun), zhaoss@jlu.edu.cn (S. Zhao).

http://dx.doi.org/10.1016/j.aeue.2017.06.026
1434-8411/

shrinkage target) [9,10]. The researches about shrinkage methods focused on finding a proper shrinkage target, and a shrinkage coefficient which should be optimal and easy to calculate. Recently, Y. Chen et al. addressed a high dimensional covariance matrix shrinkage method in the sense of minimum mean-squared-error (MSE) when the observations are Gaussian distributed [11] and elliptical distributed [12]. X. chen and Z. J. Wang introduced a shrinkage-to-tapering approach which shrinks the SCM to the tapered version by choosing some diagonals of the SCM [13]. T. Lancewicki and M. Aladjem considered a multi-target shrinkage algorithm which exploits the Ledoit-Wolf (LW) method with several targets simultaneously [14]. Most of these methods assume that the true covariance matrix likes an identity matrix, a diagonal matrix, or a diagonally dominant matrix with smoothing parameters [13–15]. Under a general assumption of the DOA estimation model, the true covariance matrix is a complex Toeplitz and Hermitian matrix with coherent entries under the uniform linear array (ULA) or other fixed structure matrices depending on the geometry of the array. Among the above mentioned methods, the diagonal matrix structure targets adopt the entries in the main diagonal of the SCM and do not contain any information about the DOAs, and the others drop some DOA information from the minor diagonals of the SCM. Hence, the current covariance matrix shrinkage methods are not suitable for the DOA estimation model. Because the shrinkage targets of these methods are not well-conditional matrices compared with the covariance matrix of the DOA estimation model.

The Toeplitz rectification is a way to improve the estimation of a covariance matrix with Toeplitz structure, which obtains a rectified SCM by averaging the entries on the diagonals of the SCM [16,17]. The R-MUSIC improved the DOA estimation of MUSIC by replacing the SCM with the Toeplitz rectified SCM. P. Vallet and P. Loubaton proved that the R-MUSIC suffers a "saturation phenomenon" that the MSE of DOA estimates will not decrease with the increase of signal-to-noise ratio (SNR) when the SNR overs a certain value [17]. Although the rectified SCM with the flaw of "saturation phenomenon", it is suitable as a shrinkage target due to its Toeplitz structure. In this paper, we consider the rectified SCM as the shrinkage target with the advantage that it contains all DOA information and provides a good DOA estimation performance at low SNR. Utilizing the unbiased and consistent estimates of the trace and moments of the Wishart distributed covariance matrix, the estimation of the shrinkage coefficient is derived as a closed form. The proposed shrinkage coefficient is inversely proportional to the SNR and tends to a stable value with the increase of the number of samples, which means when the SNR is high, the SCM accounts for a major share in the new covariance matrix estimate and the "saturation phenomenon" from the rectified SCM will be mitigated. On the contrary, the rectified SCM will play a leading role and bring a good DOA estimation performance when the SNR is low and the sample size is small.

The rest of the paper is organized as follows. The signal model, the MUSIC and G-MUSIC algorithms are presented in Section 2. The proposed covariance matrix shrinkage estimation method, the application in the MUSIC and the statistical analysis of the shrinkage coefficient estimate are introduced in Section 3. Numerical simulation results are shown in Section 4. The principal conclusion is summarized in Section 5.

Notation. In the following, we depict vectors in lowercase boldface letters and matrices in uppercase boldface. The transpose operator and conjugate transpose operator are denoted as $(\cdot)^T$ and $(\cdot)^H$, respectively. $Tr(\cdot)$, $E\{\cdot\}$ and $\|\cdot\|_F$ are the trace, the mathematical expectation and the Frobenius norm, respectively.

2. The signal model, MUSIC and G-MUSIC algorithms

2.1. The signal model

In consideration of a ULA of M sensors with half-wavelength element separation receiving K narrow-band spatially incoherent signals from directions $\{\theta_1,\ldots,\theta_K\}$, at discrete time n, the received sample vector $\boldsymbol{y}(n)\in\mathbb{C}^{M\times 1}$ is usually modeled as

$$\begin{aligned}\boldsymbol{y}(n)&=\sum_{k=1}^{K}\boldsymbol{a}(\theta_k)s_k(n)+\boldsymbol{w}(n)\\&=\boldsymbol{A}\boldsymbol{s}(n)+\boldsymbol{w}(n),\end{aligned}\tag{1}$$

where $\boldsymbol{A}=[\boldsymbol{a}(\theta_1),\ldots,\boldsymbol{a}(\theta_K)]\in\mathbb{C}^{M\times K}$ is the steering matrix with unit norm steering vectors $\boldsymbol{a}(\theta_k)=\frac{1}{\sqrt{M}}[1,e^{j\pi\sin\theta_k},\ldots,e^{j\pi(M-1)\sin\theta_k}]^T$, $k=1,\ldots,K$, and $\boldsymbol{s}(n)=[s_1(n),\ldots,s_K(n)]^T\in\mathbb{C}^{K\times 1}$ contains source signals, and $\boldsymbol{w}(n)\in\mathbb{C}^{M\times 1}$ is the additive noise. We assume there are N samples collected in the sample matrix

$$\boldsymbol{Y}_N=\boldsymbol{A}\boldsymbol{S}_N+\boldsymbol{W}_N,\tag{2}$$

where $\boldsymbol{Y}_N=[\boldsymbol{y}(1),\ldots\boldsymbol{y}(N)],\boldsymbol{S}_N=[\boldsymbol{s}(1),\ldots\boldsymbol{s}(N)]$, and $\boldsymbol{W}_N=[\boldsymbol{w}(1),\ldots\boldsymbol{w}(N)]$. We consider common assumptions of the model as following.

A 1. The signals are independent with mean $E\{s_k(n)\}=0$, $k=1,\ldots,K$ and covariance matrix $E\{\boldsymbol{s}(n)\boldsymbol{s}^H(n)\}\triangleq\boldsymbol{P}_s$.

A 2. $\boldsymbol{w}(n)$ is the complex white Gaussian noise with zero mean and unknown power σ^2, i.e. $E\{\boldsymbol{w}(n)\boldsymbol{w}^H(n)\}=\sigma^2\boldsymbol{I}_M$, where $\boldsymbol{I}_M$ is an $M\times M$ identity matrix. The noise is independent of the signals.

A 3. The number of sources K is known and satisfies $K<min(M,N)$.

Under the assumptions, the true covariance matrix of the observation vector $\boldsymbol{y}(n)$ is

$$\boldsymbol{R}=E\{\boldsymbol{y}(n)\boldsymbol{y}^H(n)\}=\boldsymbol{A}\boldsymbol{P}_s\boldsymbol{A}^H+\sigma^2\boldsymbol{I}_M.\tag{3}$$

We denote the eigenvalues of $\boldsymbol{R}$ as $\lambda_1\leqslant\lambda_2\leqslant\cdots\leqslant\lambda_M$ with the corresponding eigenvectors $\boldsymbol{e}_1,\ldots,\boldsymbol{e}_M$. The sample covariance matrix (SCM) $\boldsymbol{S}=\frac{1}{N}\boldsymbol{Y}_N\boldsymbol{Y}_N^H$is the classical maximum likelihood estimation of $\boldsymbol{R}$, but in this paper we consider an unbiased estimate

$$\hat{\boldsymbol{S}}=\frac{1}{N-1}\boldsymbol{Y}_N\boldsymbol{Y}_N^H.\tag{4}$$

The eigenvalues and eigenvectors of $\hat{\boldsymbol{S}}$ are denoted as $\hat{\lambda}_1\leqslant\hat{\lambda}_2\leqslant\cdots\leqslant\hat{\lambda}_M$ and $\hat{\boldsymbol{e}}_1,\ldots,\hat{\boldsymbol{e}}_M$, respectively, also called as sample eigenvalues and sample eigenvectors. Consequently, the DOA estimation is to infer the parameters $\theta_k,k=1,\ldots,K$ from the noisy observation matrix $\boldsymbol{Y}_N$.

2.2. The MUSIC and G-MUSIC algorithms

Under the Assumptions A1–A3, the MUSIC algorithm is based on the fact that $\theta_1,\ldots,\theta_K$ are the zeros of the pseudo-spectrum function

$$\eta_{MUSIC}(\theta)=\boldsymbol{a}^H(\theta)\boldsymbol{\Pi}\boldsymbol{a}(\theta),\tag{5}$$

where $\boldsymbol{\Pi}=\sum_{m=1}^{M-K}\boldsymbol{e}_m\boldsymbol{e}_m^H$ is the orthogonal projection matrix onto the kernel of $\boldsymbol{A}\boldsymbol{P}_s\boldsymbol{A}^H$, and also called as "noise subspace projection matrix" [3]. The unknown matrix $\boldsymbol{\Pi}$ is usually obtained by computing the eigenvectors associated with the $M-K$ smallest eigenvalues of the SCM, i.e. $\hat{\boldsymbol{\Pi}}_{SCM}=\sum_{m=1}^{M-K}\hat{\boldsymbol{e}}_m\hat{\boldsymbol{e}}_m^H$. The original MUSIC estimates

$\theta_1, \ldots, \theta_K$ by finding the K most significant minima of the following cost function

$$\hat{\eta}_{MUSIC}(\theta) = \boldsymbol{a}^H(\theta)\hat{\boldsymbol{\Pi}}_{SCM}\boldsymbol{a}(\theta). \quad (6)$$

The G-MUSIC is proposed by X. Mestre et al. and is a modified MUSIC method under the asymptotic condition of $M, N \to \infty$ with $M/N \to c \in (0, \infty)$ [8]. The G-MUSIC replaces $\hat{\boldsymbol{\Pi}}_{SCM}$ with a new estimate which is a weighted form of the quadratics of all sample eigenvectors. The cost function of the G-MUSIC is

$$\hat{\eta}_{G-MUSIC}(\theta) = \mathbf{a}^H(\theta)\sum_{m=1}^{M}\hat{\phi}(m)\hat{\mathbf{e}}_m\hat{\mathbf{e}}_m^H\mathbf{a}(\theta), \quad (7)$$

and

$$\hat{\phi}(m) = \begin{cases} 1 + \sum_{k=M-K+1}^{M}\left(\frac{\hat{\lambda}_k}{\hat{\lambda}_m - \hat{\lambda}_k} - \frac{\hat{\mu}_k}{\hat{\lambda}_m - \hat{\mu}_k}\right), & m \leqslant M-K \\ -\sum_{k=1}^{M-K}\left(\frac{\hat{\lambda}_k}{\hat{\lambda}_m - \hat{\lambda}_k} - \frac{\hat{\mu}_k}{\hat{\lambda}_m - \hat{\mu}_k}\right), & m > M-K \end{cases}, \quad (8)$$

where $\hat{\mu}_1 < \hat{\mu}_2 < \cdots < \hat{\mu}_M$ are the real-valued solutions to the following equation in $\hat{\mu}$

$$\frac{1}{M}\sum_{k=1}^{M}\frac{\hat{\lambda}_k}{\hat{\lambda}_k - \hat{\mu}} = \frac{1}{c_N}, \quad (9)$$

where $c_N = M/N$ is a substitute of the parameter c of the asymptotic condition. It is noted that when $M > N$, there will be $\hat{\lambda}_k = 0$ for $1 \leqslant k \leqslant M-N$ due with the SCM with the rank N. Hence, only N solutions of (9) are different from zero and the solutions are written as $0 = \hat{\mu}_1 = \cdots = \hat{\mu}_{M-N} < \hat{\mu}_{M-N+1} < \cdots < \hat{\mu}_M$.

3. The proposed covariance matrix estimation and DOA estimation

3.1. The proposed covariance matrix shrinkage estimation

In this section, we demonstrate the proposed covariance matrix shrinkage estimation algorithm based on the linear shrinkage estimation model [11–14]. The goal of the covariance matrix shrinkage estimation is to find an estimate $\hat{\boldsymbol{R}}$ for the unknown $\boldsymbol{R}$, and $\hat{\boldsymbol{R}}$ is the solution to

$$\begin{aligned} &\arg\min_{\rho} E\{\|\hat{\boldsymbol{R}} - \boldsymbol{R}\|_F^2\}, \\ &\quad s.t.\ \hat{\boldsymbol{R}} = (1-\rho)\hat{\boldsymbol{S}} + \rho\hat{\boldsymbol{F}}, \rho \in [0,1], \end{aligned} \quad (10)$$

where $\hat{\boldsymbol{F}}$ and ρ are the shrinkage target and shrinkage coefficient, respectively.

In the proposed method, the shrinkage target $\hat{\boldsymbol{F}}$ is set as a Toeplitz rectification matrix which is realized by averaging the diagonals of $\hat{\boldsymbol{S}}$. Let $\boldsymbol{J}^m$ be an $M \times M$ shift matrix, whose only entries of the m-th diagonal are nonzero and equal to 1. For an $M \times M$ matrix $\boldsymbol{X}$, we define $\mathscr{T}(\boldsymbol{X})$ as the Toeplitz rectification transformation

$$\mathscr{T}(\boldsymbol{X}) = \sum_{m=-(M-1)}^{M-1}\frac{1}{M-|m|}Tr(\boldsymbol{X}\boldsymbol{J}^m)\boldsymbol{J}^{-m}, \quad (11)$$

where $\boldsymbol{J}^{-m}$ stands for $(\boldsymbol{J}^m)^T$, and $\boldsymbol{J}^0 = \boldsymbol{I}_M$ [17]. Hence, the shrinkage target in (10) can be represented as

$$\hat{\boldsymbol{F}} = \mathscr{T}(\hat{\boldsymbol{S}}) = \sum_{m=-(M-1)}^{M-1}\frac{1}{M-|m|}Tr(\hat{\boldsymbol{S}}\boldsymbol{J}^m)\boldsymbol{J}^{-m}. \quad (12)$$

The optimal weight ρ is computed by differentiating (10), and the generic solution of ρ is

$$\rho = \frac{E\{Tr[\hat{\boldsymbol{S}}(\hat{\boldsymbol{S}} - \hat{\boldsymbol{F}})]\} - E\{Tr[\boldsymbol{R}(\hat{\boldsymbol{S}} - \hat{\boldsymbol{F}})]\}}{E\{Tr[(\hat{\boldsymbol{S}} - \hat{\boldsymbol{F}})^2]\}}. \quad (13)$$

To obtain an effective and simple estimation of ρ, we consider the unbiased estimations of the terms in (13) as following [15]

$$E\{Tr[\hat{\boldsymbol{S}}(\hat{\boldsymbol{S}} - \hat{\boldsymbol{F}})]\} \approx Tr[\hat{\boldsymbol{S}}(\hat{\boldsymbol{S}} - \hat{\boldsymbol{F}})] \quad (14)$$

and

$$E\{Tr[(\hat{\boldsymbol{S}} - \hat{\boldsymbol{F}})^2]\} \approx Tr[(\hat{\boldsymbol{S}} - \hat{\boldsymbol{F}})^2]. \quad (15)$$

The asymptotically unbiased estimation of $E\{Tr[\boldsymbol{R}(\hat{\boldsymbol{S}} - \hat{\boldsymbol{F}})]\}$ is computed based on $E\{\hat{\boldsymbol{S}}\} = \boldsymbol{R}$ and $E\{Tr(\hat{\boldsymbol{S}})\} = Tr(\boldsymbol{R})$. M. S. Srivastava showed the unbiased and consistent estimations of $Tr(\boldsymbol{R})$ and $Tr(\boldsymbol{R}^2)$ are [18]

$$Tr(\boldsymbol{R}) \approx Tr(\hat{\boldsymbol{S}}) \quad (16)$$

and

$$Tr(\boldsymbol{R}^2) \approx \frac{(N-1)^2}{(N-2)(N+1)}[Tr(\hat{\boldsymbol{S}}^2) - \frac{1}{N-1}Tr^2(\hat{\boldsymbol{S}})]. \quad (17)$$

The second part in the numerator in (13) can be re-written as

$$\begin{aligned} E\{Tr[\boldsymbol{R}(\hat{\boldsymbol{S}} - \hat{\boldsymbol{F}})]\} &= Tr(\boldsymbol{R}E\{\hat{\boldsymbol{S}} - \hat{\boldsymbol{F}}\}) = Tr(\boldsymbol{R}E\{\hat{\boldsymbol{S}}\}) - Tr(\boldsymbol{R}E\{\hat{\boldsymbol{F}}\}) \\ &= Tr(\boldsymbol{R}E\{\hat{\boldsymbol{S}}\}) - \sum_{m=-(M-1)}^{M-1}\frac{1}{M-|m|}E\{Tr(\hat{\boldsymbol{S}}\boldsymbol{J}^m)\}Tr(\boldsymbol{R}\boldsymbol{J}^{-m}) \\ &\approx Tr(\boldsymbol{R}^2) - \sum_{m=-(M-1)}^{M-1}\frac{1}{M-|m|}Tr(\hat{\boldsymbol{S}}\boldsymbol{J}^m)Tr(\hat{\boldsymbol{S}}\boldsymbol{J}^{-m}) \\ &= \frac{(N-1)^2}{(N-2)(N+1)}[Tr(\hat{\boldsymbol{S}}^2) - \frac{1}{N-1}Tr^2(\hat{\boldsymbol{S}})] - Tr(\hat{\boldsymbol{S}}\hat{\boldsymbol{F}}). \end{aligned} \quad (18)$$

Substituting (14), (15) and (18) to (13), after simplification we obtain the estimation of the shrinkage coefficient

$$\hat{\rho} = \frac{(N-3)Tr(\hat{\boldsymbol{S}}^2) + (N-1)Tr^2(\hat{\boldsymbol{S}})}{(N-2)(N+1)Tr[(\hat{\boldsymbol{S}} - \hat{\boldsymbol{F}})^2]}. \quad (19)$$

Then the proposed covariance matrix shrinkage estimate is

$$\hat{\boldsymbol{R}}^* = (1-\hat{\rho}^*)\hat{\boldsymbol{S}} + \hat{\rho}^*\sum_{m=-(M-1)}^{M-1}\frac{1}{M-|m|}Tr(\hat{\boldsymbol{S}}\boldsymbol{J}^m)\boldsymbol{J}^{-m}, \quad (20)$$

where $\hat{\rho}^*$ satisfies $\hat{\rho}^* = \min(\hat{\rho}, 1)$.

3.2. The application in MUSIC and the analysis of the shrinkage coefficient

We denote the eigenvalues and the associated eigenvectors of $\hat{\boldsymbol{R}}^*$ as $\hat{l}_1 \leqslant \hat{l}_2 \leqslant \cdots \leqslant \hat{l}_M$ and $\hat{\boldsymbol{u}}_1, \ldots, \boldsymbol{u}_M$, respectively. The unknown noise subspace in the MUSIC pseudo-spectrum function can be re-estimated as

$$\hat{\boldsymbol{\Pi}}_{shrinkage} = \sum_{m=1}^{M-K}\hat{\boldsymbol{u}}_m\hat{\boldsymbol{u}}_m^H. \quad (21)$$

The cost function based on the proposed covariance matrix shrinkage estimate (indicated as shrinkage-MUSIC) is

$$\hat{\eta}_{shrinkage-MUSIC}(\theta) = \boldsymbol{a}^H(\theta)\hat{\boldsymbol{\Pi}}_{shrinkage}\boldsymbol{a}(\theta). \quad (22)$$

In addition, the R-MUSIC is also a modified MUSIC which replaces the SCM in MUSIC by the rectified SCM [17]. It is noted that the shrinkage-MUSIC will become the original MUSIC when $\hat{\rho}^* = 0$ and turn into the R-MUSIC when $\hat{\rho}^* = 1$.

The R-MUSIC performs well at low SNR but suffers the "saturation phenomenon" at high SNR [17]. However, the original MUSIC works well in the case of high SNR with sufficient samples. The shrinkage estimate $\hat{\boldsymbol{R}}^*$ is a compromise between $\hat{\boldsymbol{S}}$ and $\hat{\boldsymbol{F}}$, so the ideal status is that the estimate $\hat{\boldsymbol{R}}^*$ tends to $\hat{\boldsymbol{F}}$ when the SNR is low and tends to $\hat{\boldsymbol{S}}$ when the SNR is high. That is, the shrinkage coefficient $\hat{\rho}$ should decrease with the increase of SNR. Using the results about the Wishart distributed matrices [19,20], the optimal shrinkage coefficient ρ_o and the expectation of $\hat{\rho}$ are calculated as (the details of the computing process are in the appendix)

$$\begin{aligned}\rho_o &= \frac{E\{Tr[\hat{\boldsymbol{S}}(\hat{\boldsymbol{S}}-\hat{\boldsymbol{F}})]\} - E\{Tr[\boldsymbol{R}(\hat{\boldsymbol{S}}-\hat{\boldsymbol{F}})]\}}{E\{Tr[(\hat{\boldsymbol{S}}-\hat{\boldsymbol{F}})^2]\}} \\ &= \frac{Tr^2(\boldsymbol{R}) + Tr(\boldsymbol{R}^2) - \Delta_1}{NTr(\boldsymbol{R}^2) + Tr^2(\boldsymbol{R}) - \Delta_2}\end{aligned} \tag{23}$$

and

$$\begin{aligned}E\{\hat{\rho}\} &= E\left\{\frac{(N-3)Tr(\hat{\boldsymbol{S}}^2) + (N-1)Tr^2(\hat{\boldsymbol{S}})}{(N-2)(N+1)Tr[(\hat{\boldsymbol{S}}-\hat{\boldsymbol{F}})^2]}\right\} \\ &= \frac{Tr^2(\boldsymbol{R}) + Tr(\boldsymbol{R}^2)}{NTr(\boldsymbol{R}^2) + Tr^2(\boldsymbol{R}) - \Delta_2},\end{aligned} \tag{24}$$

where $\Delta_1 = \sum_{m=-(M-1)}^{M-1} \frac{1}{M-|m|}[Tr(\boldsymbol{RJ}^m\boldsymbol{RJ}^{-m}) + Tr(\boldsymbol{RJ}^{-m}\boldsymbol{RJ}^{-m})]$ and $\Delta_2 = \sum_{m=-(M-1)}^{M-1} \frac{1}{M-|m|}[(N-1)Tr(\boldsymbol{RJ}^m)Tr(\boldsymbol{RJ}^{-m}) + Tr(\boldsymbol{RJ}^m\boldsymbol{RJ}^{-m}) + Tr(\boldsymbol{RJ}^{-m}\boldsymbol{RJ}^{-m})]$. The bias of $\hat{\rho}$ is

$$\begin{aligned}bias(\hat{\rho}) &= E\{|\hat{\rho} - \rho_o|\} \\ &= \frac{\Delta_1}{NTr(\boldsymbol{R}^2) + Tr^2(\boldsymbol{R}) - \Delta_2}.\end{aligned} \tag{25}$$

There is a deviation between $\hat{\rho}$ and ρ_o. Hence, $\hat{\rho}$ is a biased estimation in the case of finite sample size. The deviation leads that $\hat{\rho}$ can not tend to zero when the SNR is high enough, which is shown in Fig. 1. The relationship between $\hat{\rho}$ and N is shown by simulations and the results are shown in Fig. 2. $\hat{\rho}$ decreases and tends to a stable value with the increase of N. The theory analysis and simulation present that $\hat{\rho}$ is sensitive to the SNR, but not sensitive to N.

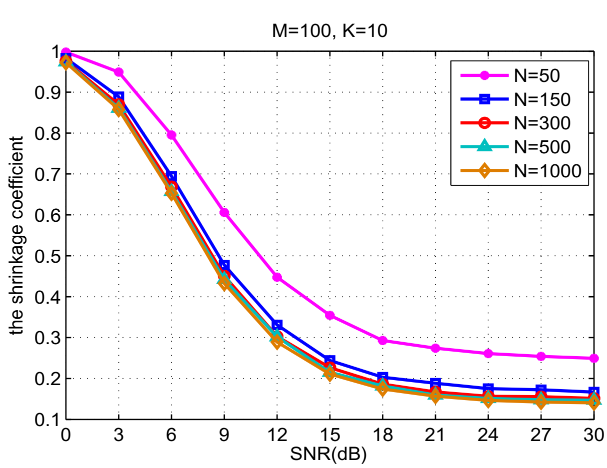

Fig. 1. The empirical mean of shrinkage coefficient estimates versus SNR with the sample size $N = 50, 150, 300, 500, 1000$, and other parameters are $M = 100$ and $K = 10$.

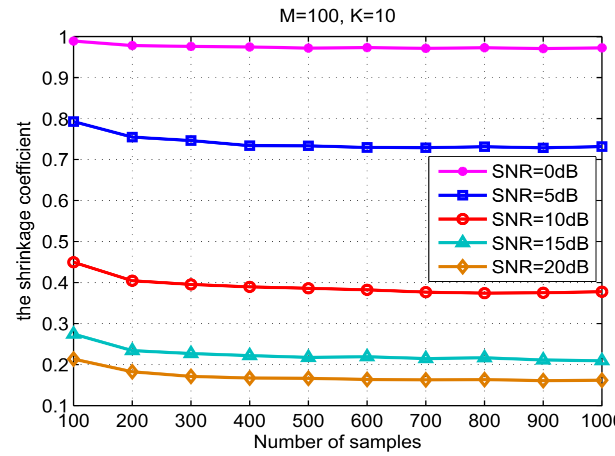

Fig. 2. The empirical mean of shrinkage coefficient estimators versus the number of samples at the different SNR, and other parameters are $M = 100$ and $K = 10$.

4. Numerical simulations

The statistical properties of the proposed shrinkage coefficient estimate are shown in Figs. 1 and 2. The performances of DOA estimation of the shrinkage-MUSIC, MUSIC, R-MUSIC and G-MUSIC are shown in Figs. 3–6. In all simulations, the source signals with identical power p_s are generated by mutually independent AR (1) Gaussian sequences with model parameter 0.9. The additive noise is the white Gaussian noise with mean zero and power $\sigma^2 = 1$. The SNR is given by

$$SNR = 10\lg(p_s/\sigma^2). \tag{26}$$

The definition of the RMSE of DOA estimates is

$$RMSE(\hat{\theta}) = \sqrt{\frac{1}{IK}\sum_{i=1}^{I}\sum_{k=1}^{K}|\hat{\theta}_{ki} - \theta_k|^2}, \tag{27}$$

where $\hat{\theta}_{ki}$ is the estimate of θ_k in the i^{th} simulation and I is the number of the Monte Carlo simulations. All simulation results are calculated from 500 independent numerical trials, i.e. $I = 500$.

In Figs. 1 and 2, there are ten signals from DOAs $\{-55^\circ, -43^\circ, -31^\circ, -19^\circ, -7^\circ, 5^\circ, 17^\circ, 29^\circ, 41^\circ, 53^\circ\}$ impinging on a ULA with $M = 100$. The empirical mean of $\hat{\rho}_i^*$ is calculated by $\bar{\rho}^* = \frac{1}{I}\sum_{i=1}^{I}\hat{\rho}_i^*$. Fig. 1 presents $\bar{\rho}^*$ versus the SNR with different N. Fig. 2 presents $\bar{\rho}^*$ versus N at different SNR. The curves in Fig. 1 confirm that $\hat{\rho}^*$ is inversely proportional to the SNR. When the SNR is low, $\hat{\rho}^*$ closes or equals to 1 and the rectified SCM accounts for a considerable proportion in the proposed covariance matrix estimate. On the contrary, the SCM plays a major role in the proposed covariance matrix estimate when the SNR is high. The curves in Fig. 2 confirm that when the SNR is fixed, $\hat{\rho}^*$ decreases and tends to a stable value with the increase of the number of samples. It illustrates that $\hat{\rho}^*$ is changed obviously with the change of SNR, and is influenced weakly by the number of samples.

In Figs. 3 and 4, four spatially separated signals from DOAs $\{-10^\circ, 10^\circ, 25^\circ, 40^\circ\}$ arrive a ULA with $M = 30$. The grid of the spectral peak searching is 0.02°. Figs. 3 and 4 show the RMSEs of the spatially separated DOA estimates versus SNR and N, respectively. In Fig. 3, the "saturation phenomenon" of the R-MUSIC occurs at SNR = 9 dB and the shrinkage-MUSIC mitigates the effect. Although the shrinkage-MUSIC performs weaker than G-MUSIC and MUSIC when SNR$\geqslant$15 dB, the RMSE of DOA estimation of the shrinkage-MUSIC is less than 0.04° and is small enough for source location. The shrinkage-MUSIC can not "switch" to the original MUSIC at high SNR with the reason that $\hat{\rho}$ is a biased estimate

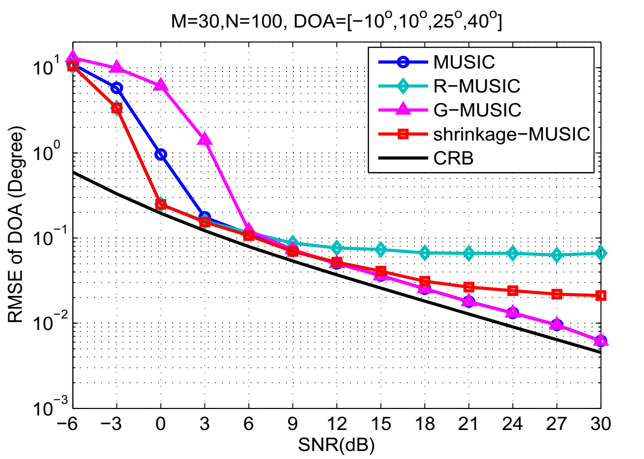

Fig. 3. The RMSE of spatially separated DOA estimators of the MUSIC, R-MUSIC, G-MUSIC and shrinkage-MUSIC versus SNR, and other parameters are $M = 30$, $N = 100$ and $K = 4$.

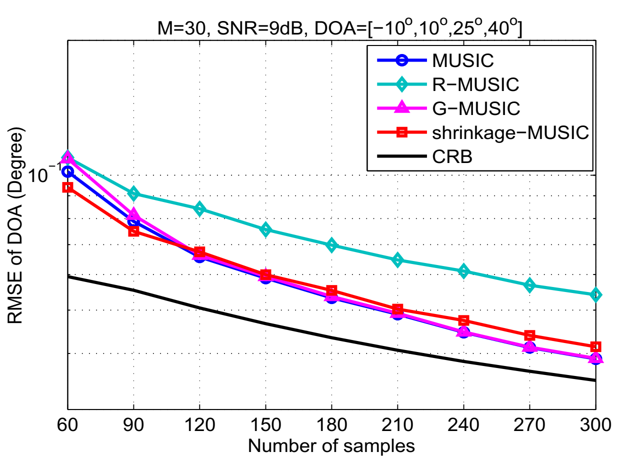

Fig. 4. The RMSE of spatially separated DOA estimators of the MUSIC, R-MUSIC, G-MUSIC and shrinkage-MUSIC versus the number of samples, and other parameters are SNR = 9 dB, $M = 30$ and $K = 4$.

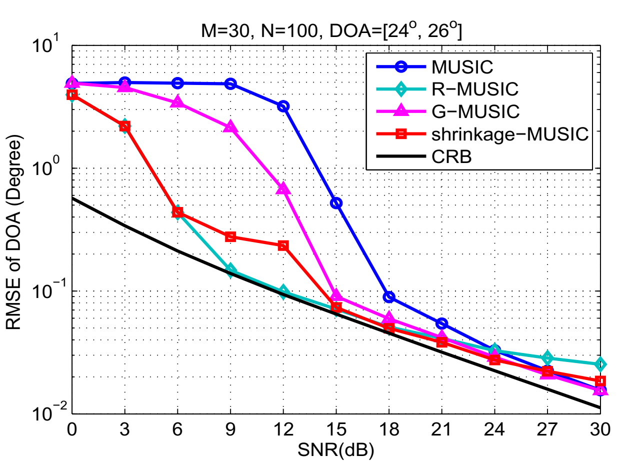

Fig. 5. The RMSE of closely spaced DOA estimators of the MUSIC, R-MUSIC, G-MUSIC and shrinkage-MUSIC versus SNR, and other parameters are $M = 30$, $N = 100$ and $K = 2$.

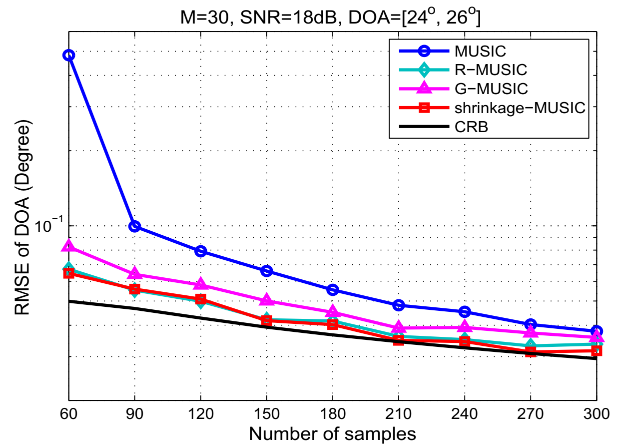

Fig. 6. The RMSE of closely spaced DOA estimators of the MUSIC, R-MUSIC, G-MUSIC and shrinkage-MUSIC versus the number of samples, and other parameters are SNR = 18 dB, $M = 30$ and $K = 2$.

and can not tend to zero when the SNR is high enough. Fig. 4 illustrates that if the R-MUSIC in the "saturated state", the increase of N can not remove this phenomenon. However, the shrinkage-MUSIC realizes a better or a similar performance compared with the MUSIC and the G-MUSIC. Figs. 3 and 4 confirm that $\hat{\rho}^{*}$ improves the estimation of the covariance matrix and makes an improvement of the DOA estimation to some extent.

In Figs. 5 and 6, two closely spaced signals from DOAs $\{24^{\circ}, 26^{\circ}\}$ arrive a ULA with $M = 30$. The grid of the spectral peak searching is also 0.02°. Fig. 5 presents the RMSE of the two spatially closed DOA estimates versus SNR with $N = 100$. When SNR$\leqslant$15 dB, the R-MUSIC has the best performance and the shrinkage-MUSIC is the second-best among of the four methods. The "threshold value" of the MUSIC occurs at SNR = 18 dB when estimating the two closed spatially DOAs. When the SNR is higher than 21 dB, the shrinkage-MUSIC and the R-MUSIC perform weaker but sightly compared with MUSIC and G-MUSIC. The performance of shrinkage-MUSIC is better than the R-MUSIC and close to the G-MUSIC in the case of high SNR. Fig. 6 shows the RMSE of two spatially closed DOA estimates versus N at SNR = 18 dB. The results of Fig. 6 show that when the SNR is over the "threshold value", the small sample size makes much negative effect on the MUSIC and G-MUSIC than the R-MUSIC and shrinkage-MUSIC.

5. Conclusion

In this paper, we have proposed a covariance matrix shrinkage method to improve the DOA estimation under a uniform linear array in the case of a large number of sensors with relatively few samples. The estimation of the covariance matrix is realized via the linear shrinkage algorithm with a Toeplitz rectified sample covariance matrix (SCM) as the shrinkage target. The shrinkage coefficient estimate is derived as a closed form, which makes the proposed covariance matrix estimate to be a good compromise between the SCM and the rectified SCM with a theoretical guarantee. Moreover, the proposed covariance matrix estimate applied in the MUSIC can provide some advantages compared with the MUSIC, R-MUSIC and G-MUSIC methods.

Acknowledgments

We are grateful to the editor and reviewers for their helpful comments and suggestions, which have led to significant improvements of this article. This work was supported by the National Natural Science Foundation of China (Grant No. 61171137) and the National Major Research and Development Program of China (Grand No. 2016YFB1001304).

Appendix A

In Section 2, the true covariance matrix is $\boldsymbol{R} = E\{\boldsymbol{y}(n)\boldsymbol{y}^H(n)\} = \boldsymbol{AP}_s\boldsymbol{A}^H + \sigma^2\boldsymbol{I}_M$, and the sample vector $\boldsymbol{y}(n)$ is of the Gaussian distribution with $\boldsymbol{y}(n) \sim \mathcal{N}(\boldsymbol{0}, \boldsymbol{R})$. The $M \times M$ random matrix $\boldsymbol{W} = \sum_{n=1}^{N} \boldsymbol{y}(n)\boldsymbol{y}^H(n)$ has a complex Wishart distribution with N degrees of freedom and parameter matrix $\boldsymbol{R}$, i.e., $\boldsymbol{W} \sim \mathscr{W}_M^{\mathbb{C}}(N, \boldsymbol{R})$ [19,20]. So the SCM is of the complex Wishart distribution $(N-1)\hat{\boldsymbol{S}} \sim \mathscr{W}_M^{\mathbb{C}}(N, \boldsymbol{R})$. The results about the moments of Wishart distributed matrices used in this paper are

$$E\{Tr(\hat{\boldsymbol{S}})\} = Tr(\boldsymbol{R}), \tag{28}$$

$$E\{Tr(\hat{\boldsymbol{S}}^2)\} = \frac{N}{N-1} Tr(\boldsymbol{R}^2) + \frac{1}{N-1} Tr^2(\boldsymbol{R}), \tag{29}$$

and

$$E\{Tr(\boldsymbol{D}\hat{\boldsymbol{S}})Tr(\boldsymbol{B}\hat{\boldsymbol{S}})\} = Tr(\boldsymbol{DR})Tr(\boldsymbol{BR}) + \frac{1}{N-1} Tr(\boldsymbol{DRBR}) + \frac{1}{N-1} Tr(\boldsymbol{D}^T\mathbf{RBR}), \tag{30}$$

where $\boldsymbol{B}$ and $\boldsymbol{D}$ are $M \times M$ constant matrices. Hence, there are

$$E\{Tr^2(\hat{\boldsymbol{S}})\} = Tr^2(\boldsymbol{R}) + \frac{2}{N-1} Tr(\boldsymbol{R}^2), \tag{31}$$

$$\begin{aligned} E\{Tr(\hat{\boldsymbol{S}}\hat{\boldsymbol{F}})\} &= \sum_{m=-(M-1)}^{M-1} \frac{E\{Tr(\hat{\boldsymbol{S}}\boldsymbol{J}^m)Tr(\hat{\boldsymbol{S}}\boldsymbol{J}^{-m})\}}{M-|m|} \\ &= \sum_{m=-(M-1)}^{M-1} \frac{1}{M-|m|} [Tr(\boldsymbol{RJ}^m)Tr(\boldsymbol{RJ}^{-m}) \\ &\quad + \frac{1}{N-1} Tr(\boldsymbol{RJ}^m\boldsymbol{RJ}^{-m}) + \frac{1}{N-1} Tr(\boldsymbol{RJ}^{-m}\boldsymbol{RJ}^{-m})], \end{aligned} \tag{32}$$

and

$$\begin{aligned} E\{Tr(\hat{\boldsymbol{F}}^2)\} &= \sum_{m=-(M-1)}^{M-1} \sum_{n=-(M-1)}^{M-1} \frac{E\{Tr(\hat{\boldsymbol{S}}\boldsymbol{J}^m)Tr(\hat{\boldsymbol{S}}\boldsymbol{J}^n)\}Tr(\boldsymbol{J}^{-m}\boldsymbol{J}^{-n})}{(M-|m|)(M-|n|)} \\ &= \sum_{m=-(M-1)}^{M-1} \sum_{n=-(M-1)}^{M-1} \frac{Tr(\boldsymbol{J}^{-m}\boldsymbol{J}^{-n})}{(M-|m|)(M-|n|)} [Tr(\boldsymbol{RJ}^m)Tr(\boldsymbol{RJ}^n) \\ &\quad + \frac{1}{N-1} Tr(\boldsymbol{RJ}^m\boldsymbol{RJ}^n) + \frac{1}{N-1} Tr(\boldsymbol{RJ}^{-m}\boldsymbol{RJ}^n)] \\ &= \sum_{m=-(M-1)}^{M-1} \frac{1}{M-|m|} [Tr(\boldsymbol{RJ}^m)Tr(\boldsymbol{RJ}^{-m}) \\ &\quad + \frac{1}{N-1} Tr(\boldsymbol{RJ}^m\boldsymbol{RJ}^{-m}) + \frac{1}{N-1} Tr(\boldsymbol{RJ}^{-m}\boldsymbol{RJ}^{-m})] \\ &= E\{Tr(\hat{\boldsymbol{S}}\hat{\boldsymbol{F}})\}. \end{aligned} \tag{33}$$

Substituting (31)–(33) into ρ and $E\{\hat{\rho}\}$, there are

$$\begin{aligned} \rho &= \frac{E\{Tr[\hat{\boldsymbol{S}}(\hat{\boldsymbol{S}} - \hat{\boldsymbol{F}})]\} - E\{Tr[\boldsymbol{R}(\hat{\boldsymbol{S}} - \hat{\boldsymbol{F}})]\}}{E\{Tr[(\hat{\boldsymbol{S}} - \hat{\boldsymbol{F}})^2]\}} \\ &= \frac{Tr^2(\boldsymbol{R}) + Tr(\boldsymbol{R}^2) - \Delta_1}{NTr(\boldsymbol{R}^2) + Tr^2(\boldsymbol{R}) - \Delta_2} \triangleq \rho_o \end{aligned} \tag{34}$$

and

$$\begin{aligned} E\{\hat{\rho}\} &= E\left\{\frac{(N-3)Tr(\hat{\boldsymbol{S}}^2) + (N-1)Tr^2(\hat{\boldsymbol{S}})}{(N-2)(N+1)Tr[(\hat{\boldsymbol{S}} - \hat{\boldsymbol{F}})^2]}\right\} \\ &= E\left\{\frac{(N-3)Tr(\hat{\boldsymbol{S}}^2) + (N-1)Tr^2(\hat{\boldsymbol{S}})}{(N-2)(N+1)[Tr(\hat{\boldsymbol{S}}^2) - Tr(\hat{\boldsymbol{S}}\hat{\boldsymbol{F}})]}\right\} \\ &= \frac{Tr^2(\boldsymbol{R}) + Tr(\boldsymbol{R}^2)}{NTr(\boldsymbol{R}^2) + Tr^2(\boldsymbol{R}) - \Delta_2}, \end{aligned} \tag{35}$$

where $\Delta_1 = \sum_{m=-(M-1)}^{M-1} \frac{1}{M-|m|} [Tr(\boldsymbol{RJ}^m\boldsymbol{RJ}^{-m}) + Tr(\boldsymbol{RJ}^{-m}\boldsymbol{RJ}^{-m})]$ and $\Delta_2 = \sum_{m=-(M-1)}^{M-1} \frac{1}{M-|m|} [(N-1)Tr(\boldsymbol{RJ}^m)Tr(\boldsymbol{RJ}^{-m}) + Tr(\boldsymbol{RJ}^m\boldsymbol{RJ}^{-m}) + Tr(\boldsymbol{RJ}^{-m}\boldsymbol{RJ}^{-m})]$.

References

[1] Chang JC, Chang AC. DOA estimation in the time space CDMA system using modified particle swarm optimization. AEU-Int J Electron Commun 2013;67(4):340–7. http://dx.doi.org/10.1016/j.aeue.2012.10.003.

[2] Cui K, Wu W, Huang J, Chen X, Yuan N. Doa estimation of lfm signals based on stft and multiple invariance esprit. AEU-Int J Electron Commun 2017;77:10–7. http://dx.doi.org/10.1016/j.aeue.2017.04.021.

[3] Schmidt R. Mutiple emitter location and signal parameter estimation. IEEE Trans Antennas Propagat 1986;34(3):276–80. http://dx.doi.org/10.1109/TAP.1986.1143830.

[4] Poormohammad S, Farzaneh F. Precision of direction of arrival (doa) estimaiton using novel three dimensional array geometries. AEU-Int J Electron Commun 2017;75:35–45. http://dx.doi.org/10.1016/j.aeue.2017.02.013.

[5] Johnson BA, Abramovich YI, Mestre X. MUSIC, G-MUSIC, and Maximum-likelihood performance breakdown. IEEE Trans Signal Process 2008;56(8):3944–58. http://dx.doi.org/10.1109/TSP.2008.921729.

[6] Paul D, Aue A. Random matrix theory in statistics: a review. J Stat Plan Inference 2014;150:1–29. http://dx.doi.org/10.1016/j.jspi.2013.09.005.

[7] Mestre X. On the asymptotic behavior of the sample estimates of eigenvalues and eigenvectors of covariance matrices. IEEE Trans Signal Process 2008;56(11):5353–68. http://dx.doi.org/10.1109/TSP.2008.929662.

[8] Mestre X, Lagunas MA. Modified subspace algorithms for DOA estimation with large arrays. IEEE Trans Signal Process 2008;56(2):598–614. http://dx.doi.org/10.1109/TSP.2007.907884.

[9] Ledoit O, Wolf M. A well-conditioned estimator for large dimensional covariance matrices. J Multivar Anal 2004;88(2):365–411. http://dx.doi.org/10.1016/S0047-259X(03)00096-4.

[10] Bodnar T, Gupta AK, Parolya N. On the strong covergence of the optimal linear shrinkage estimator for large dimensional covariance matrix. J Multivar Anal 2014;132(2):215–28. http://dx.doi.org/10.1016/j.jmva.2014.08.006.

[11] Chen Y, Wiesel A, Eldar YC, Hero AO. Shrinkage algorithms for MMSE covariance estimation. IEEE Trans Signal Process 2010;58(10):5016–28. http://dx.doi.org/10.1109/TSP.2010.2053029.

[12] Chen Y, Wiesel A, Hero AO. Robust shrinkage estimation of high-dimensional covariance matrices. IEEE Trans Signal Process 2011;59(9):4097–107. http://dx.doi.org/10.1109/SAM.2010.5606730.

[13] Chen X, Wang ZJ, Mckeown MJ. Shrinkage-to-tapering estimation of large covariance matrices. IEEE Trans Signal Process 2012;60(11):5640–56. http://dx.doi.org/10.1109/TSP.2012.2210546.

[14] Lancewicki T, Aladjem M. Multi-target shrinkage estimation for covariance matrices. IEEE Trans Signal Process 2014;62(44):6380–90. http://dx.doi.org/10.1109/TSP.2014.2364784.

[15] Ikeda Y, Kubokawa T, Srivastava MS. Comparison of linear shrinkage estimators of a large covariance matrix in normal and non-normal distributions. Comput Stat Data Anal 2016;95:95–108. http://dx.doi.org/10.1109/ICASSP.2016.7472582.

[16] Forster P. Generalized rectification of cross spectral matrices for arrays of arbitrary geometry. IEEE Trans Signal Process 2001;49(5):972–8. http://dx.doi.org/10.1109/78.917801.

[17] Vallet P, Loubaton P. Toeplitz rectification and DOA estimation with MUSIC. In: Proc. int. conf. acoustics, speech and signal processing (ICASSP), Florence; May 2014. p. 2237–41. http://dx.doi.org/10.1109/ICASSP.2014.6853997.

[18] Srivastava MS, Yanagihara H, Kubokawa T. Tests for covariance matrices in high dimension with less sample size. J Multi Anal 2014;130:289–309. http://dx.doi.org/10.1016/j.jmva.2014.06.003.

[19] Letac G, Massam H. All invariant moments of the Wishart distribution. Scand J Stat 2004;31(2):295–318. http://dx.doi.org/10.1111/j.1467-9469.2004.01-043.x.

[20] Graczyk P, Letac G, Massam H. The complex Wishart distribution and the symmetric group. Ann Stat 2003;31(1):287–309. http://dx.doi.org/10.1214/aos/1046294466.